

Mechanically-Controlled Spectroscopic Imaging for Tissue Classification

Laura Connolly^a, Tamas Ungi^a, Andras Lasso^a, Thomas Vaughan^a, Mark Asselin^a, Parvin Mousavi^b, Scott Yam^c, Gabor Fichtinger^a

^aLaboratory for Percutaneous Surgery, School of Computing, Queen's University, Kingston, Canada

^bMedical Informatics Laboratory, School of Computing, Queen's University, Kingston, Canada

^cSchool of Electrical and Computer Engineering, Queen's University, Kingston, Canada.

ABSTRACT

PURPOSE: Raman Spectroscopy is amongst several optical imaging techniques that have the ability to characterize tissue non-invasively. To use these technologies for intraoperative tissue classification, fast and efficient analysis of optical data is required with minimal operator intervention. Additionally, there is a need for a reliable database of optical signatures to account for variable conditions. We developed a software system with an inexpensive, flexible mechanical framework to facilitate automated scanning of tissue and validate spectroscopic scans with histologic ground truths. This system will be used, in the future, to train a machine learning algorithm to distinguish between different tissue types using Raman Spectroscopy.

METHODS: A sample of chicken breast tissue is mounted to a microscope slide following a biopsy of fresh frozen tissue. Landmarks for registration and evaluation are marked on the specimen using a material that is recognizable in both spectroscopic and histologic analysis. The slides are optically analyzed using our software. The landmark locations are extracted from the spectroscopic scan of the specimen using our software. This information is then compared to the landmark locations extracted from images of the slide using the software, ImageJ.

RESULTS: Target registration error of our system in comparison to ImageJ was found to be within 1.1 mm in both x and y directions.

CONCLUSION: We demonstrated a system that can employ accurate spectroscopic scans of fixed tissue samples. This system can be used to spectroscopically scan tissue and validate the results with histology images in the future.

KEYWORDS: Raman Spectroscopy, optical imaging, automated scanning, 3D printer, tissue classification, optical signature.

1. INTRODUCTION

Raman Spectroscopy is a technology in the field of optical image analysis that offers promise for cancer diagnosis and imaging. This method of optical tissue analysis is based on the unique Raman shift by localized molecules upon incident photon excitation [1].

Studies in the literature suggest that the Raman shift of malignant tissue demonstrates a unique spectroscopic profile compared to that of healthy tissue and can help accomplish accurate differentiation of cancerous and benign samples [1], [2]. An example of differences in the spectroscopic signatures between tissues types can be seen in Figure 1. Here, the unprocessed Raman signatures of two tissue samples are shown for skin cells versus store-bought tissue (collected using BWTek i-Raman Plus 785S). It is important to note the unique spectroscopic profile of each sample. This technique can be used for real time intraoperative margin assessment by offering noninvasive, high-speed tissue classification. Raman Spectroscopy could therefore be used to prevent re-excision and recurrence of the disease in cancer surgery patients.

The Raman shift of molecules is dependent on a variety of factors including incident wavelength intensity, spot size, integration time and signal to noise ratio [3]. As such, there has been difficulty demonstrating consistent Raman signatures of real tissue *in vivo* [3]. There is currently no documented database of the Raman spectra of malignant tissue specimens available for reference. The Raman spectrum must be analyzed by an experienced user before any

conclusions about the tissue can be made. Therefore, in order for a Raman probe to be used for real time intraoperative margin assessment, it will require a sophisticated machine learning algorithm to assist in this analysis. Training this algorithm will, in turn, need a reliable scanning system capable of automating the process for numerous training cases.

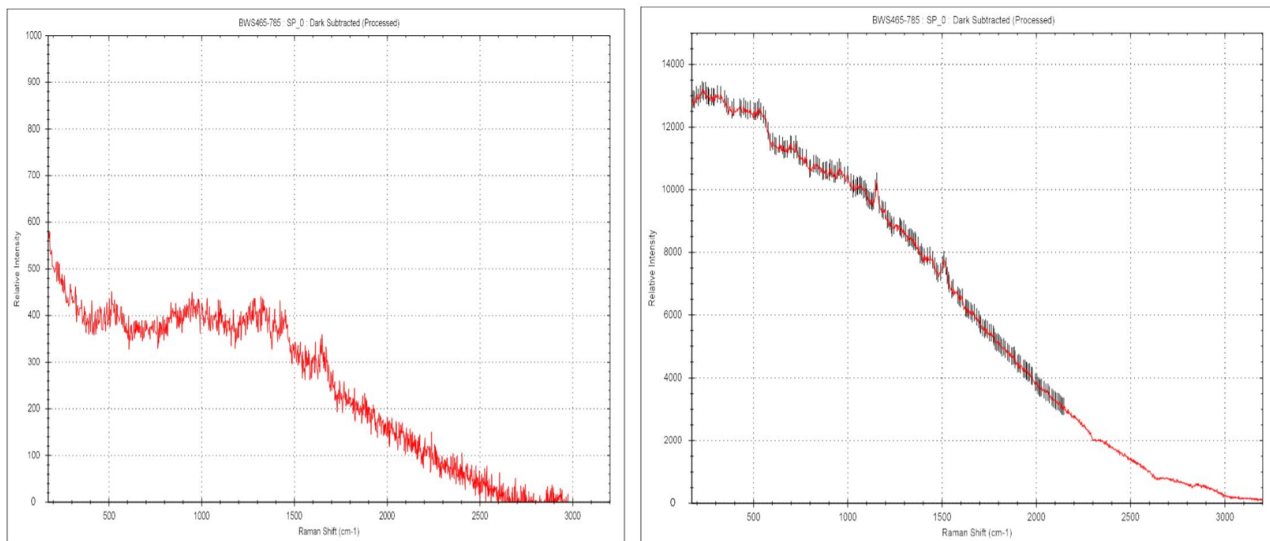


Figure 1- *Left:* Raman shift of dead skin. *Right:* Raman shift of store-bought tissue. Note that both samples were taken at an integration time of 500 ms, single shot, excitation wavelength of 785 nm and about 300 mW. The x-axis represents the Raman shift in cm⁻¹ and the y-axis represents the relative intensity.

We propose an automated system that can be used for optical scanning and their validation with ground truth histology, in an effort to create data to train machine learning algorithms. Our system is integrated with an open source platform, 3D Slicer (www.slicer.org) in order to demonstrate superposition of microscopic and spectroscopic images in the same coordinate space. The tools within the software will be used in the future to verify the spectroscopic conclusions and construct a dependable database of optical signatures for various tissue types.

2. MATERIALS AND METHODS

2.1 System Overview

The system is developed using a modified Monoprice Mini V2 3D printer to operate as an automated translation stage for a 660 nm LED probe connected to a ThorLabs CCD Compact Spectrometer. The extruder head is removed from the original printer and replaced with the aforementioned probe (Figure 2). The heating beds and fan are also disconnected from the printer.

The Monoprice Mini V2 3D printer was chosen as the mechanical framework because it operates in an x, y and z coordinate system that can be used to communicate locational information about the mechanical head. This 3D printer responds to a programming language called G – code which corresponds to a specific set of commands and positioning information that relies on the internal coordinate system of the 3D printer. Our model system is an affordable 3D printer that is widely accessible and adaptable to various optical imaging devices. Any local embodiment of this system can be used to house other optical imaging devices by simply replacing the adapter head and probe.

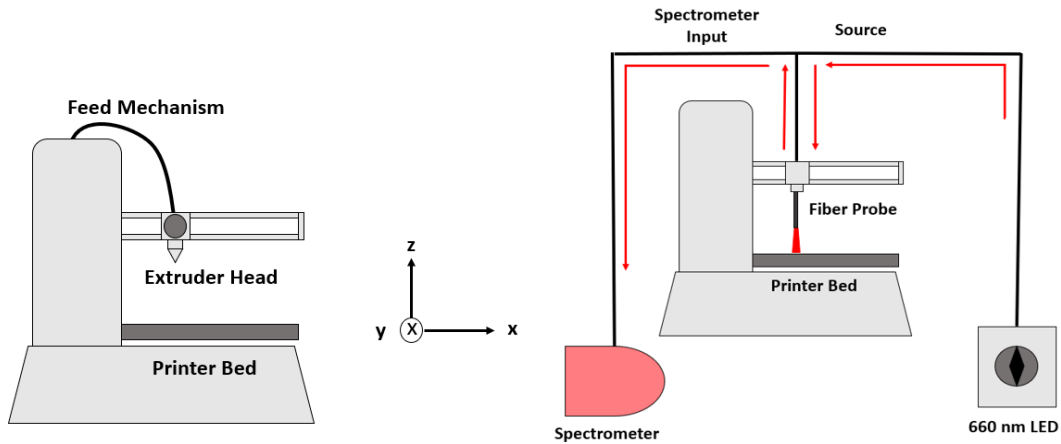


Figure 2- *Left:* Schematic diagram of the original 3D printer before any alterations were made. *Right:* Schematic diagram of the adapted 3D printer with the LED probe and spectrometer in place of the extruder head. Red arrows are used to demonstrate the path of light.

Data integration, streaming and processing between the 3D printer and spectrometer is performed with PLUS (Public software Library for Ultrasound imaging research) toolkit (www.plustoolkit.org) [4]. Integration with 3D Slicer is performed using the Slicer OpenIGTLink interface (www.openIGTLink.org) and the PLUS server launcher [4], [5]. Data analysis is performed using the Slicer IGT Modules (www.slicerigt.org) [6]. The following diagram (Figure 3) outlines the hierarchy of hardware and software used for this system and includes some of the specific Slicer and SlicerIGT modules used in this application. Some of these modules include MarkupsToModel to visualize the spectroscopic scans in the 3D Slicer display window, Fiducial Registration Wizard to facilitate registration, and Spectrum Viewer to determine the spectrum threshold of the specimen of interest.

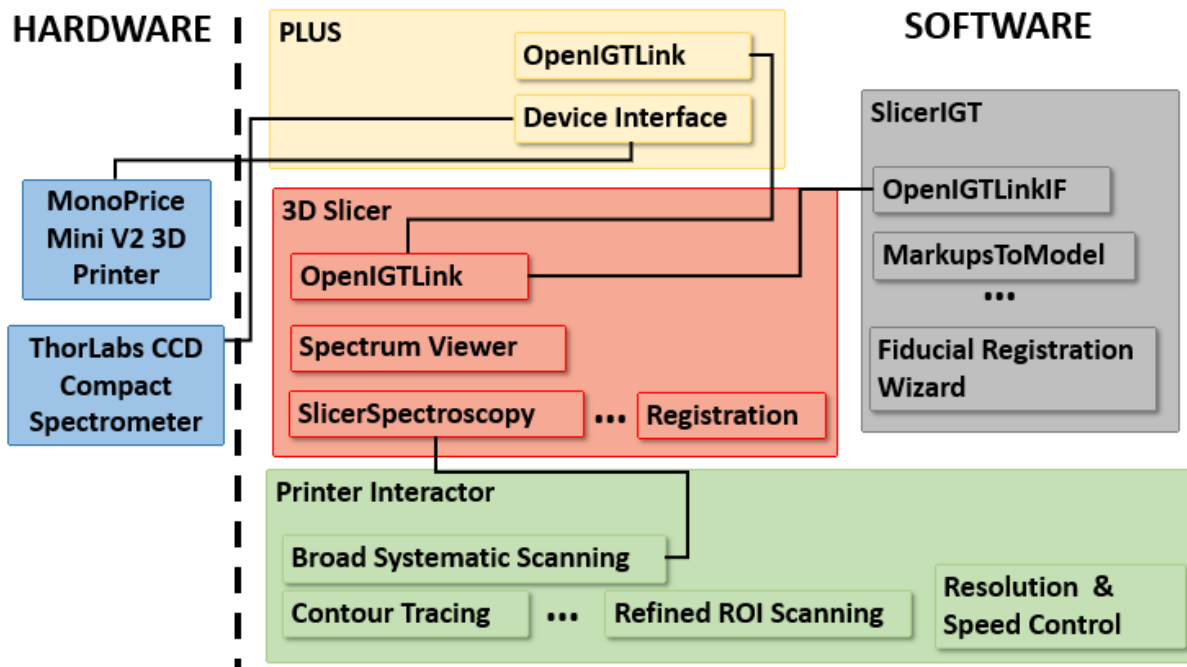


Figure 3- Hierarchical order of the software and hardware components used for the development of our system.

2.2 Registration of Optical Scans to Histology

We developed a tool to enable image registration and validate the results of the optical scans with histology. Within the image registration capability, the user can manually manipulate the platform of the 3D printer using the arrow keys on their keyboard. This function is useful for moving towards a particular region of interest (ROI) in which a landmark for registration is known to be located. With that, the user can manually place markers in 3D slicer with reference to the probe to distinguish points to be used for registration. The user can later load the histology image to register it to optical scans to verify and learn from the spectrum. Learning from the specimen will enable the user to establish a relationship between the spectroscopic and histologic results.

2.3 Basic Scanning System

The MPV2 3D Printer is 120 mm wide in both the x and y directions. This printer has a resolution of 100 microns [7]. The systematic scanning module is a user interface for scanning resolution and speed control. This module initiates a systematic scan of the entire printer bed by moving the probe in a rectangular grid pattern at the specified resolution and speed. Spectrum recognition for this paper is computed by comparing the entire live spectrum to a reference spectrum that is collected before the scanning begins. The module performs spectrum analysis at the speed specified by a user, and places a marker in the 3D viewer if the live spectral data matches the reference spectra within a specified threshold. A threshold of 10 W/m^2 (the difference in intensity values of the live spectra from the reference spectra) is used to determine whether or not the live spectra is dark or light. This was found to be the boundary point between the opaque and transparent components of the specimen we tested. The software will iteratively compare the live spectra to the reference spectra by computing the intensity differences. In the future, when this system is used to train a Raman probe, the spectrum will have to be collected and saved at each point and registered to histology images before any spectrum analysis is computed. This will allow the user to compile and save data at specific coordinates for further analysis.

After scanning, the registration tool within the software in conjunction with 3D Slicer can be used to verify the spectrum analysis with their corresponding histological ground truth. This validation is necessary in order to develop a reliable database of optical signatures.

2.4 System Optimization

A limitation of optical scanning using the proposed framework is the time cost of facilitating data fusion, controlled mechanical positioning and spectra analysis synchronously. An ROI scanning capability is implemented to mitigate this cost. Using the keyboard controls, the user is able to manually mark distinct ROI boundaries on the printer bed in which a refined systematic scan can be performed. This capability can be used independently when the user is confident in the selected ROI boundary or following a broad systematic search to refine a specific area of interest. The system allows the user to search this region in a rectilinear or diagonal pattern (Figure 4). The diagonal scanning pattern is used for this paper.

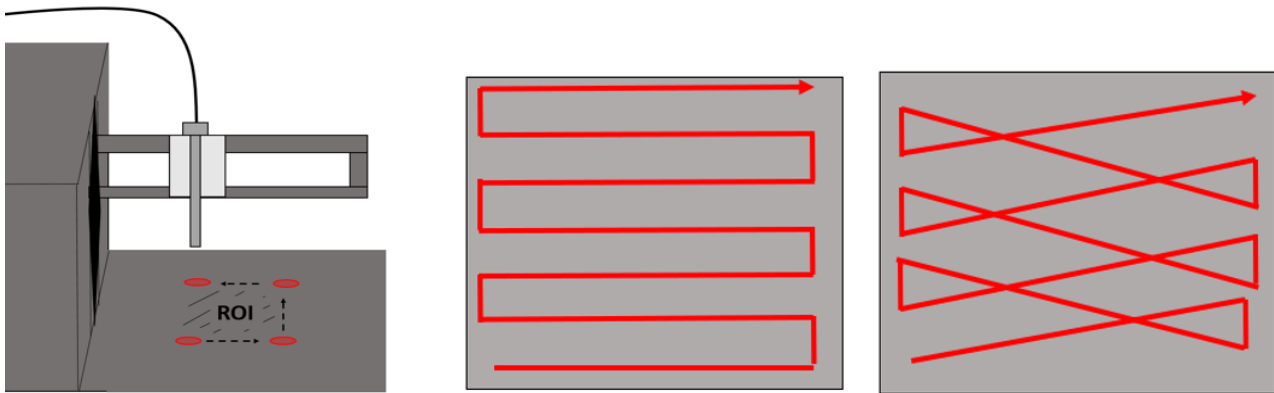


Figure 4- *Left:* ROI boundary definition. *Middle:* Rectilinear scanning pattern. *Right:* Diagonal scanning pattern.

Two contour tracing algorithms are also available within the software if the user is interested in defining a contour and not an entire area. The first algorithm determines the convex hull of the boundary points of a systematic scan. The second approach operates based on quadrant checking and can be used independent of any systematic scanning. In this approach, the sample under the probe is assessed at a user-specified resolution, and the trajectory to follow is determined based on the pattern observed (Figure 5). For example, as seen in Figure 5 (1), the probe starts at the bottom left corner of the boundary and moves in four directions at the specified resolution (right, down, left, up in 2-6, respectively). Depending on the quadrant(s) where the subject is observed, it moves in that direction for the next scanning step.

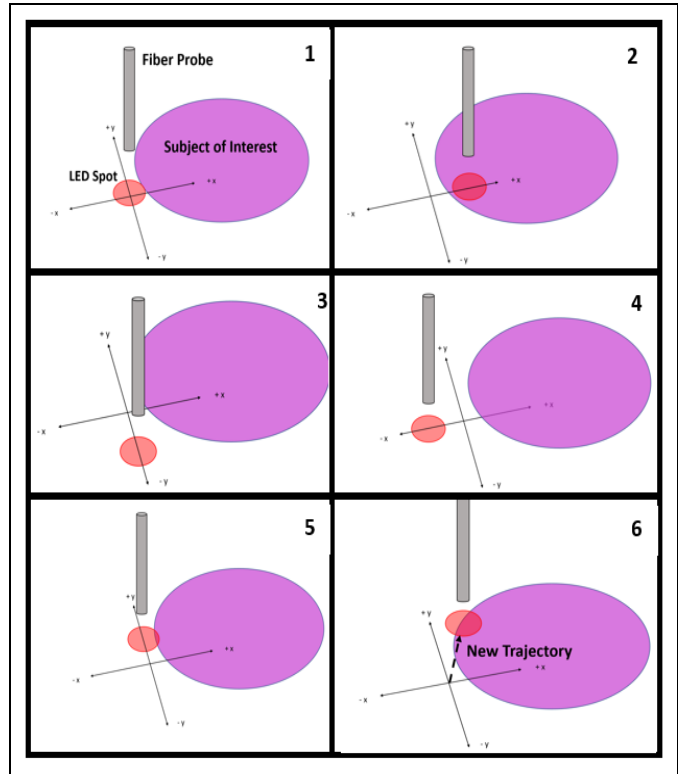


Figure 5- Independent contour tracing scheme. (1) The probe starts at the bottom left corner of the boundary and moves in four directions at the specified resolution, (2-6) right, down, left, up in 2-6, respectively. Depending on the quadrant(s) where the subject is observed, the probe moves in that direction for the next scanning step.

Contour tracing is implemented in a variety of ways to allow the user to define specific boundaries with or without a refined area scan. This capability has the potential to be used to mark and outline an area of interest by replacing the fiber probe with a marker or pen. With an adapted framework, this technology could be used in surgical planning.

2.5 Data

To demonstrate this scanning system, a sample of chicken breast tissue is histologically analyzed following a frozen section protocol, and scanned with our system. This protocol is typically used to analyze the histology samples of excised tissue and to determine resection margins of a tumor excision [8]. After the sample has been frozen in temperatures below -20° C, it is sectioned into thin slices [8]. These sections are then mounted to a glass slide, stained with Hematoxylin and Eosin (H&E) dye and marked with distinct registration and test points in dark ink (Figure 6).

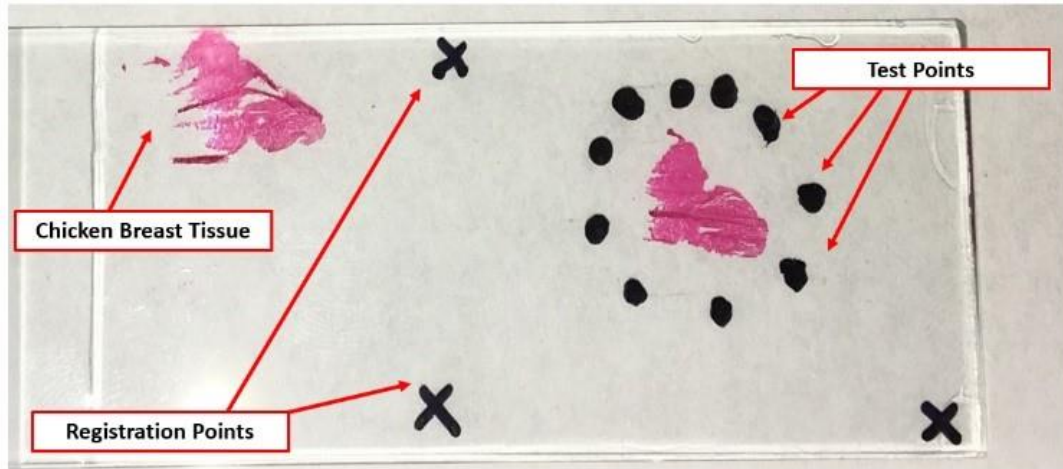


Figure 6- Mounted store-bought tissue with landmarks used as registration and test points.

The slides are then imaged microscopically to validate that the landmarks used as registration points will be visible in both spectroscopic and histology imaging (Figure 7).

2.6 Scanning Specifications

Our system was used to scan a manually selected ROI of 20x19 mm containing the test points, at 500x500 um resolution. The z axis was fixed at a height of 37 mm which meant the LED was held almost directly on the surface of the slide. The LED driver was set to 0.7 amps and has a beam width of 1.5 mm. The slide was fixed on a white background on the printer bed and analyzed with the 660 nm LED probe. At this wavelength, the probe emits a red light. This wavelength can accurately distinguish the test points from the unmarked slide surface at the threshold mentioned earlier.

A similar analysis was performed using another scientific imaging software, ImageJ (www.ImageJ.net), in order to compare the spectroscopic scan with manual identification of the landmark test points [9]. The slide is photographed with a scale to establish the correct ratio between the pixel size and the distance between each test point. From this, a set of coordinates can be extracted and landmark test locations can be compared to our system.

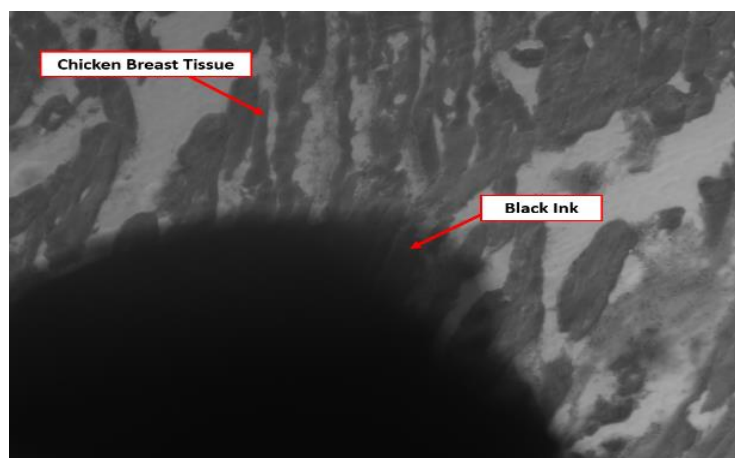


Figure 7- Microscopic Image of one of the sample slides (10x magnification). Note: this is not the same sample slide from Figure 6, this slide had a test point directly on top of the tissue.

3. RESULTS AND DISCUSSION

The test points shown in Figure 6 were distinguished spectroscopically using our software and selected manually using ImageJ based on visual inspection of a user. The resultant images can be seen in Figure 8.

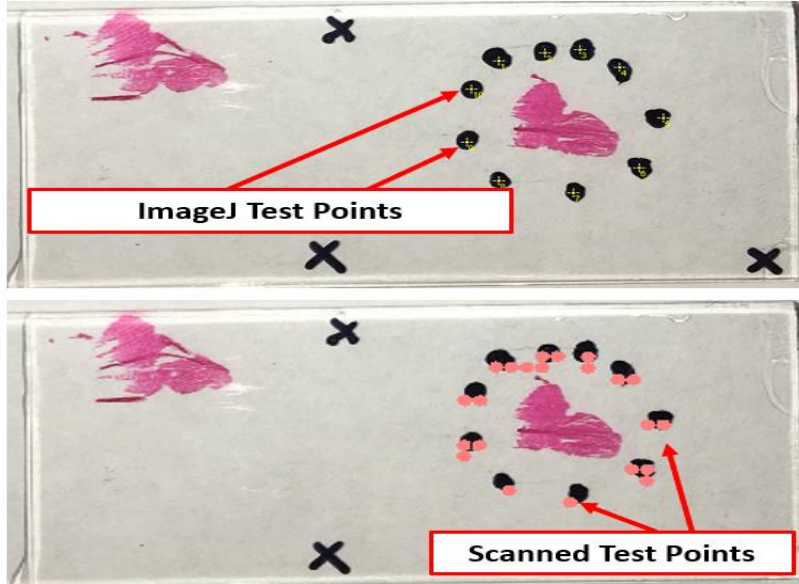


Figure 8- *Top:* Manually selected landmarks for testing from ImageJ. *Bottom:* Landmark points for testing collected from spectroscopic scan.

A similarity transform was performed in 3D Slicer to register the landmarks that were identified with our system to those selected manually with ImageJ. The fiducial registration error (FRE) is defined as the mean squared error of the distance between the registration points (shown as x in Figures 6 and 8). FRE values in x and y direction are reported in Table 1 below, indicating the close alignment of the spectroscopic scan to the ImageJ scan. For each test point (circles in Figures 6 and 8) in the spectroscopic scan, the centroid of the surrounding marked points was taken as the location. After registration, the coordinates of each test point in the spectroscopic scan were compared to the coordinates of that same point in the ImageJ scan. The average difference between those point coordinates is reflected in the target registration error (TRE) values in Table 1.

Table 1- FRE and TRE between the point coordinates identified using the 3D printer system and ImageJ.

Measured Quantity	X (mm)	Y (mm)
FRE	0.075 ± 0.04	0.17 ± 0.09
TRE	0.88 ± 0.22	1.1 ± 0.17

3.1 Proposed Work Flow

In order to train a Raman probe, the system will need a large reference database to compare the live spectrum of tissue to. This system can be used to automate the process of accurate and precise tissue scanning and registration by overlaying spectral analysis with histology imaging. With a Raman probe, the procedure will differ slightly as the tissue will be scanned with the architecture before it has been stained. Both processes are outlined in Figure 9 below.

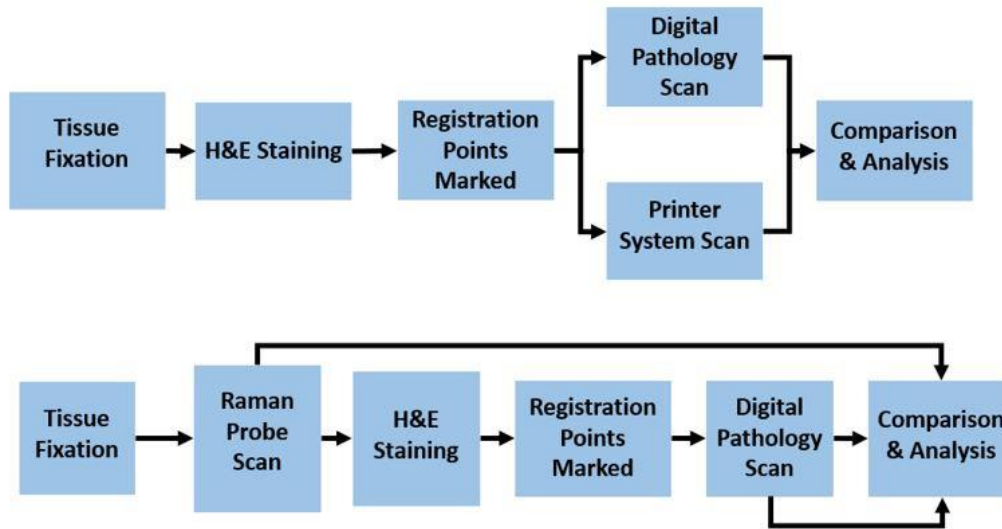


Figure 9- *Top:* Process used for this paper without Raman probe. *Bottom:* Modified process including Raman probe.

With this small modification, these same methods used to validate the software can be applied to obtain optical scans of several cancer tissue samples to further develop the application of Raman Spectroscopy for intraoperative margin assessment. Additionally, the architecture is customizable to various optical devices making it universally viable for database training and tissue distinction with any optical probe.

4. CONCLUSIONS

This scanning system is demonstrated to be within 1.1 mm of accuracy to manual selection with ImageJ. The differences between FRE and TRE values in x and y directions are 0.095 ± 0.05 mm and 0.22 ± 0.05 mm, respectively. This difference is caused by systematic scanning pattern in that the probe moves more frequently in the x direction than it does in the y directions. These results could be improved by employing the spectroscopic scans at a slower speed or modifying the scanning pattern to so that motions in both directions are as frequent. This can be achieved using the diagonal scanning pattern mentioned earlier.

The proposed system can be used as a testbed for employing spectroscopic scanning for intraoperative margin assessment. Raman Spectroscopy is a promising application for this system but a combination of technologies including Optical Coherence Tomography (OCT), ultrasound, mass spectrometry, and other systems could also benefit from this database development tool. The inexpensive, adaptable framework of the scanning system makes it a practical solution for training and testing various tissue classification technologies.

Future work on this project will include collecting and automating spectroscopic analysis using the data collected with this testbed and a machine learning algorithm. This could eliminate the need for operator intervention or expert opinion once the system is reliable enough to make accurate decisions about the tissue being assessed. The device could be used to assist in surgical excision by offering real time margin assessment.

5. NEW OR BREAKTHROUGH WORK TO BE PRESENTED

An accurate scanning system was developed to perform mechanically controlled spectroscopic scanning and validation with histology imaging for tissue classification. This system has the potential to be applied to various tissue classification techniques by collecting locational information and data for database development.

REFERENCES:

- [1] R. Manoharan *et al.*, “Raman Spectroscopy and Fluorescence Photon Migration for Breast Cancer Diagnosis and Imaging,” *Photochem. Photobiol.*, vol. 67, no. 1, pp. 15–22, Jan. 1998.
- [2] Z. Huang, A. McWilliams, H. Lui, D. I. McLean, S. Lam, and H. Zeng, “Near-infrared Raman spectroscopy for optical diagnosis of lung cancer,” *Int. J. Cancer*, vol. 107, no. 6, pp. 1047–1052, Dec. 2003.
- [3] N. Kourkoumelis, I. Balatsoukas, V. Moulia, A. Elka, G. Gaitanis, and I. D. Bassukas, “Advances in the in Vivo Raman Spectroscopy of Malignant Skin Tumors Using Portable Instrumentation.,” *Int. J. Mol. Sci.*, vol. 16, no. 7, pp. 14554–70, Jun. 2015.
- [4] A. Lasso, T. Heffter, A. Rankin, C. Pinter, T. Ungi, and G. Fichtinger, “PLUS: Open-Source Toolkit for Ultrasound-Guided Intervention Systems,” *IEEE Trans. Biomed. Eng.*, vol. 61, no. 10, pp. 2527–2537, Oct. 2014.
- [5] J. Tokuda *et al.*, “OpenIGTLink: an open network protocol for image-guided therapy environment.,” *Int. J. Med. Robot.*, vol. 5, no. 4, pp. 423–34, Dec. 2009.
- [6] T. Ungi, A. Lasso, and G. Fichtinger, “Open-source platforms for navigated image-guided interventions.,” *Med. Image Anal.*, vol. 33, pp. 181–186, Oct. 2016.
- [7] “Monoprice MP Select Mini 3D Printer V2, Black,” 2018. [Online]. Available: https://www.monoprice.com/product?c_id=107&cp_id=10724&cs_id=1072403&p_id=21711. [Accessed: 25-Jul-2018].
- [8] E. Brender, A. Burke, and R. M. Glass, “Frozen Section Biopsy,” *JAMA*, vol. 294, no. 24, p. 3200, Dec. 2005.
- [9] J. Schindelin, C. T. Rueden, M. C. Hiner, and K. W. Eliceiri, “The ImageJ ecosystem: An open platform for biomedical image analysis.,” *Mol. Reprod. Dev.*, vol. 82, no. 7–8, pp. 518–29, Jul. 2015.